# Inverse Fuzzy Fault Models for Fault Isolation and Severity Estimation in Industrial Pneumatic Valves

M.F. Ávila-Díaz[1], M.A. Márquez-Vera[1], O. Díaz-Parra[1], V. Puig[2], A. Ma'arif[3]
[1]Polytechnic University of Pachuca, Carr. Pachuca-Cd. Sahagún Km 20, Zempoala 43830, Hidalgo, Mexico
[2]Universitat Politècnica de Catalunya, Institut de Robòtica i Informàtica Industrial, Llorens i Artigas, 4-6, 08028 Barcelona, Spain
[3]Universitas Ahmad Dahlan, Jl. Kapas 9, Semaki, Kec. Umbulharjo, Yogyakarta 55166, Indonesia
E-mail: marquez@upp.edu.mx

**Keywords:** fault diagnosis, pneumatic valves, fuzzy modeling, actuator fault

**Received:** August 17, 2023

*Fault detection is crucial in the chemical industry for identifying process problems, and determining the nature of the fault is essential for scheduling maintenance. This study focuses on the application of inverse fuzzy models to reconstruct faults for the purpose of detection, isolation, and classification. By inverting fuzzy models, the fault signal can be reconstructed, enabling identification of the fault source and its characteristics. To address the issue of undetected small abrupt faults, we employed the wavelet transform. This approach allows for the detection of incipient faults, while the classification is achieved by evaluating the response of the fault reconstruction. Fault isolation is accomplished by comparing the reconstructed faults. However, in the case of the pneumatic valve utilized, four out of the 19 simulated faults demonstrated poor isolation due to the similarity of their reconstructions using inverse fuzzy models. We also present a comparison with similar applications in existing literature. The fault detection rate obtained in this study is 84.81%, which is higher compared to the rates of 55.45% and 82.37% reported in other works. Additionally, the accuracy achieved in this work is 78.85%, indicating the ratio of correctly classified faults to the total number of measurements, including both fault and no-fault conditions.*

*Povzetek: V članku je predstavljen model za zaznavanje, izolacijo in oceno napak v industrijskih pnevmatskih ventilih, ki dosega visoko uspešnost zaznavanja napak.*

## 1 Introduction

Ensuring safety is of paramount importance in the chemical industry. Various processes within this industry are susceptible to faults, which not only pose a risk to product integrity but also endanger the safety of factory operators [1]. Startling statistics from Japan reveal that over the past five years, approximately one-fourth of chemical industries reported more than 20 accidents [2]. In a comprehensive analysis of 170 accidents, [3] found that 56.2% of these cases involved explosions, including a notable incident on August 12, 2015, in Tianjin, China, which resulted in 165 fatalities and eight missing individuals. Hence, the ability to detect faults assumes paramount importance in the chemical industry [4]. Recognizing the limitations of the defense-in-depth approach in averting accidents like the Fukushima Daiichi nuclear disaster in 2011, [5] proposed implementing the safety diagnosability principle to enhance situational awareness. This approach facilitates the development of maintenance schedules for optimal operational performance and process safety [6], while also enabling timely response during emergencies.

A fault refers to an unexpected deviation in a system's behavior. The detection of faults serves as a crucial first step in fault diagnosis, indicating the presence of a problem. Subsequently, fault isolation becomes necessary to identify the specific nature of the issue. This combined process of fault detection and isolation (FDI) is often referred to as fault diagnosis in many research papers [7]. Some authors further include an identification stage to assess the magnitude of the fault. As a result, the comprehensive execution of these stages constitutes the overall fault diagnosis procedure [8].

Two main techniques are commonly employed for FDI applications. The first technique involves utilizing an approximate model to compute the discrepancy between the real process outputs and the model-derived outputs, referred to as the residual signal. The detection of faults is achieved by analyzing the magnitude of the residual signal [9]. Fault isolation, on the other hand, involves examining the fault's characteristics, such as its frequency response or employing symptom mapping from the symptom space to the fault space, as demonstrated by [8]. The second technique for fault isolation involves utilizing measured data from the process to search for discernible patterns. Statistical methods, such as Hotelling's statistic ($T^2$-chart) and the squared prediction error (Q-chart), have been employed for this purpose [10]. Additionally, fault diagno-

sis in pneumatic valves has been demonstrated using principal component analysis [11]. Alternatively, soft computing techniques like fuzzy logic and artificial neural networks (ANN) have also been utilized for fault diagnosis [12].

When sensor-measured data is utilized for FDI, the methodology is known as data-driven. This approach leverages past information on the process both with and without faults to detect and classify the presence of faults, primarily employing artificial neural networks (ANNs) [13]. Deep neural networks are particularly effective in extracting features that enhance FDI performance. For instance, in fault diagnosis of Tennessee Eastman processes, [14] employed a combination of convolutional ANNs and long short-term memory units. Similarly, [15] implemented an adaptive convolutional ANN for multiscale feature extraction in the same process.

Additionally, there are publications where system behavior analysis is employed to identify new operating points or peculiar dynamics indicative of faults, even in the absence of prior information [16]. However, it is important to note that data-driven methods, as pointed out by [17], may struggle with correlating acquired samples with unlabeled data. Moreover, [18] specified that these methods are susceptible to data sparsity and proposed the use of deep temporal clustering to address this challenge.

## 1.1 Case of study

Electro-pneumatic valves find widespread usage in industries such as chemical [19], biotechnology, food processing [20], cement production [21, 22], and energy generation [23]. These valves play a vital role in regulating fluid flow within processing pipelines. In certain industrial contexts, valves are also referred to as actuators. However, these devices can be susceptible to issues such as erosion and degradation [24, 25], which may lead to faults with potential cascading effects throughout the entire process [26]. Additionally, faults can originate from the spring component used in hydraulic valves [27].

A project called the Development and Application of Methods for Actuator Diagnosis in Industrial Control Systems (DAMADICS) was proposed to develop online diagnostic tools for a pneumatic valve, specifically simulating a sugar evaporation station in Cukrownia Lublin, Poland [9]. The purpose of the process is to maintain the syrup level between 14% and 70% for juice condensation, as a lower value can lead to overheating of the evaporation chamber, while higher values can result in contamination of other stations within the factory [28]. The developed model accurately simulates real phenomena that can potentially cause faults in the valve actuator, making it highly applicable in real-world scenarios. This platform has been utilized to develop fault detection and isolation (FDI) techniques without the need for extensive analytical knowledge of the valve or its associated faults [29].

The DAMADICS model comprises three key components: a control valve, a servomotor, and a positioner. The model incorporates five inputs: i) the control variable $C_V$, ii) the liquid pressure before the valve $P_1$, iii) the liquid pressure behind the valve $P_2$, iv) the liquid temperature $T$, and v) the faults vector $f$. The model produces two output signals: the displacement of the valve head $X$ and the liquid flow rate $F$ [28].

In this system, the linear rod motion is determined by the pressure force, which is achieved using a flexible diaphragm. The movement of the rod controls the internal area of the valve, thereby influencing the fluid force, which is dependent on the pressure difference between $P_1$ and $P_2$ [9]. A PID controller is responsible for regulating the air within the chamber to maintain a desired set point. The model has the capability to simulate 19 distinct faults, denoted as $F_1$, $F_2$, ..., $F_{19}$.

## 1.2 State of the art

Now, let's explore the state-of-the-art research in fault detection and isolation (FDI) for the DAMADICS benchmark, focusing primarily on studies that employ data-driven techniques.

The utilization of residual signals for fault detection is a widely employed approach in FDI. [30] introduced an interval model to derive nonlinear interval observers. These observers are utilized to generate residual signals for fault detection, and subsequently, the responses from a set of observers are compared to fault signatures for fault isolation. Soft computing techniques can also be employed to model nonlinear systems [31]. In model-based FDI, the evaluation of residuals plays a crucial role in fault detection, and an interesting methodology involves the implementation of fuzzy logic.

Fuzzy models were proposed by [9] to approximate the variables $X$ and $F$ by utilizing the input variables. Residual signals were employed for fault detection, followed by the use of 19 fuzzy classifiers to isolate the specific faults.

[32] improved the fuzzy partition of classifiers by incorporating clustering algorithms. Their methodology enables the detection of new operation modes in a model-free manner, meaning that it is data-driven and does not rely on prior fault information. They implemented adaptive fuzzy rules using an incremental unsupervised Gaussian participatory clustering procedure, which shows promise in terms of its ability to adapt without prior knowledge of faults.

Another approach utilizing fuzzy logic for FDI was demonstrated by [8]. In their study, they employed fuzzy generalized nearest prototype classifiers and applied 20 distinct magnitudes of faults. It is noteworthy that they developed a classifier capable of isolating different magnitudes within the same fault.

In addition, [33] utilized artificial neural networks (ANN) for FDI. They employed ANN models to represent the behavior of the DAMADICS benchmark both with and without faults in order to calculate the residuals. By evaluating the magnitude of these residuals, it becomes feasible to detect faults. For the fault isolation stage, ANN

models were utilized for each potential fault under evaluation within a specific time window. A larger time window provides higher confidence with a delay, whereas a shorter time window enables early isolation but with lower confidence.

[36] employed an ANN to develop a neural model for the DAMADICS benchmark and calculate residual signals. The fault isolation process involved utilizing a decision tree to identify unique signatures or footprints in the symptoms. This approach offered the advantage of reduced time required for FDI, and it successfully isolated 12 distinct faults.

On the other hand, [33] identified three fault groups that exhibit similar symptoms. Interestingly, even the fault-free scenario can be mistakenly isolated within these groups. Specifically, there exists a group comprising faults $F_5$, $F_8$, and $F_{14}$ as potential candidates due to their shared symptom. This similarity poses a challenge for fault isolation.

Neuro-fuzzy systems combine the computational power and learning capability of ANNs with the reasoning and interpretability of fuzzy logic [34]. These systems can be viewed as either fuzzy systems adapted as ANNs or ANNs with fuzzy sets and operators as their units [12]. In the context of the benchmark used in this study, [12] implemented multiple observers for FDI. These observers, known as unknown input observers, were combined using fuzzy logic to generate output estimates. Notably, their approach involved using the Gustafson-Kessel clustering for the initial fuzzy partition and employing genetic programming to obtain state-space subsystems as the rule consequents. Additionally, they proposed the use of one linear model to approximate $X$ and five linear submodels for $F$. Importantly, they emphasized that faults can have varying effects at different operating points. Their methodology, known as the neuro-fuzzy and decoupling fault diagnosis scheme, showed promising results.

A similar approach was demonstrated by [35], who utilized an ANN model to approximate the process behavior. Subsequently, a neuro-fuzzy classifier was employed to detect and isolate faults based on the residual signals. This method follows a model-based approach, and it successfully detected and isolated two specific faults.

[37] introduced a pattern-recognition approach using radial basis function networks for classification. The results were then aggregated using a fuzzy system to generate a decision signal. In their study, they successfully isolated faults $F_1$, $F_2$, $F_7$, $F_8$, $F_{10} - F_{13}$, and $F_{15} - F_{19}$ in abrupt scenarios.

Self-organizing maps (SOM), similar to ANN, have been utilized by [38] for fault diagnosis. In their approach, fault detection is achieved by computing the difference between the obtained signals and the healthy behavior of DAMADICS. However, it should be noted that some faults were undetectable using this method. A significant drawback of this approach is the considerable time required for online diagnosis. Another application of SOM for fault classification was demonstrated by [39], where they successfully classified three faults, even in cases where fault classes overlapped.

An insightful overview of computational intelligence techniques applied in FDI was presented by [40]. They explored the application of various techniques such as fuzzy logic, ANNs, neuro-fuzzy systems, and genetic algorithms in FDI for diverse systems, including gas turbines, conductive flow systems, and aero-engines. In particular, Chapter 1 of [41] highlights the significance of FDI in industrial processes and discusses the utilization of computational intelligence techniques to address challenges such as local nonlinearities, noise, and uncertainty.

A distinct approach was introduced by [42], where FDI was tackled by verifying the consistency of the current fault identification with a specific fault set using timed automata. This approach does not necessitate prior information about the system. The faults considered in this study were $F_{16}$, $F_{18}$, and $F_{19}$, and they were successfully isolated after 16 sample times in the DAMADICS simulation. Another application of fault detection was presented by [43], where a methodology called "typically and eccentricity data analysis" was employed for online fault detection without the need for prior knowledge of the system. The obtained results showcased a true positive rate (fault detection rate) of 74.96% for faults $F_{16} - F_{19}$.

Wear and tear on systems can lead to the development of incipient faults, and they can also provide insights into the actuator's remaining lifespan [44]. Detecting incipient faults can be challenging as they may resemble modifications in the operating point. Early detection is crucial for such faults since they exhibit a continuous and gradual development that may only be detectable when their magnitude approaches 50%. [28] employed a hidden Markov model to detect both abrupt faults (sudden appearance) and incipient faults. This data-driven methodology utilized 46 distinct symbols to differentiate between different operating conditions.

In a review conducted by Capaci et al. [29], the authors explored the field of smart diagnosis in control valves, focusing on the analysis of both normal and abnormal operating conditions. The study examined various statistical and soft computing techniques to compare and analyze the results obtained from these conditions. The review aimed to provide insights into the effectiveness of different diagnostic approaches in detecting and characterizing valve abnormalities.

Table 1 lists the characteristics of works mentioned above indicating advantages and limitations found for FDI in the DAMADICS benchmak.

In this work, we detect, isolate, and classify faults in the DAMADICS benchmark by reconstructing the faults using inverse fuzzy models. While model-based FDI typically relies on observers and residual signals for fault evaluation, the main contribution of this paper is the utilization of inverse models to directly identify the fault responsible for the system behavior without the need for computing residuals. To enhance fault isolation, the faults are grouped into

Table 1: Related works for FDI.

| Reference | Methodology | Advantages | Limitations |
|---|---|---|---|
| [30] | Nonlinear observers | Good detection | Time required for residual evolution, not all faults can be isolated. |
| [9] | Fuzzy models | Automation of fuzzy rules | Fault detection and isolation, to use uncertain information. |
| [32] | Clustering | Not to require prior information | Fault diagnosis free of model. |
| [8] | Fuzzy classifier | To isolate the fault magnitude | Computational effort to develop the classifier. |
| [33] | Artificial neural networks | To improve the fault detection rate or to accelerate the detection time | To collect data for the ANN model, more design to isolate incipient faults. |
| [35] | Neuro-fuzzy systems | Good detection | Cannot be applied for unknown working conditions, unknown faults cannot be isolated. |
| [12] | Neuro-fuzzy systems | Detection independent to the fault magnitude | To know the noise distribution |
| [36] | ANN and decision trees | Fast isolation using past information | To collect data for the ANN model |
| [37] | Radial-basis functions and fuzzy logic | Temporally informative features with little computational cost. | Average results. |
| [38] | Self-organizing maps | Classification even with overlapped faults | Some undetectable faults, Time consuming. |
| [39] | Self-organizing maps | To isolate and identify faults without a data preprocessing | Time consuming. |
| [42] | Timed automata | Not to require prior information | Only three faults were diagnosed. |
| [43] | Typicality and eccentricity data analytics | Precision average = 83.30% | Problems to detect incipient faults. |
| [28] | Hidden Markov model | Early detection | Only three faults were detected. |

classes based on their source, and we employed the wavelet transform to highlight incipient faults. The remaining sections of this paper are organized as follows: Section 2 describes the DAMADICS system used as the benchmark for FDI. Section 3 presents the methodology used, including the obtention of fuzzy models (subsection 3.1) and the explanation of how to invert the fuzzy models (subsection 3.2). The results are presented in Section 4, with fault detection results shown in subsection 4.1 and fault isolation presented in subsection 4.2. A comparison with similar applications is also included in the discussion Section 5. Finally, conclusions are provided in Section 6.

# 2 Benchmark description

The DAMADICS benchmark model, developed by the Research Training Network of the European Commission during the 2000-2004 period under the Framework 5 Human Potential Programme, provides a simulation of the flow dynamics through a valve. The flow rate is determined by the position of a rod, as the rod's movement regulates the flow area inside the valve [20]. This valve, known as an electro-pneumatic actuator, plays a crucial role in controlling the flow through the pipeline installation. It consists of a plate connected to the chamber walls through a flexible diaphragm. The position of the rod is determined by a control signal, which, depending on its value, either connects the chamber with the pneumatic circuit or with the atmosphere. To achieve linear motion of the servomotor stem, a compressible fluid-powered device operates on the flexible diaphragm [20]. To correct any mispositions caused by disturbances, a positioner is employed in the system.

The DAMADICS model offers the capability to simulate 19 different faults, which are listed in Table 2 of [8]. The model itself can be downloaded from `http://diag.mchtr.pw.edu.pl/damadics/`. Notably, the model allows for the simulation of incipient faults, which can often be mistaken for changes in the operating point. These incipient faults can also be utilized to predict the lifespan of industrial actuators [45]. Figure 11 of [20] presents a fault scheme specific to the DAMADICS actuator, illustrating the origin of the faults and the variables involved in identifying each fault. The faults can manifest as either stationary events, such as abrupt faults, or non-stationary signals like random or incipient variations in the values of the supply pressure (fault $F_{16}$) [46].

The faults in the DAMADICS benchmark can be simulated with various magnitudes, although some of them can only be simulated in an abrupt form. It is important to note that certain cases in Table 3 do not have a physical interpretation and, as a result, were not considered for simulation. These excluded cases may involve faults that are not practically feasible or do not align with real-world scenarios. It is essential to focus on the faults that have meaningful interpretations and are relevant to the system under consideration.

In the study shown in [8], a table was presented that pro-

Table 2: Faults in the DAMADICS model.

| Fault origin | Fault | Description | Simulation values |
|---|---|---|---|
| Control valve | $F_1$ | Valve clogging | [0, 1] |
| | $F_2$ | Valve sedimentation | [0, 1] |
| | $F_3$ | Valve erosion | [0, 1] |
| | $F_4$ | Brushing friction | [-1, 1] |
| | $F_5$ | External leakage | [0, 1] |
| | $F_6$ | Internal leakage | [0, 1] |
| | $F_7$ | Critical flow | [0, 1] |
| Servomotor | $F_8$ | Twisted servomotor's rod | [0, 1] |
| | $F_9$ | Terminals tightness | [0, 1] |
| | $F_{10}$ | Servomotor's diaphragm perforation | [0, 1] |
| | $F_{11}$ | Servomotor's spring fault | [0, 1] |
| Positioner | $F_{12}$ | Electro-pneumatic transducer fault | [-1, 1] |
| | $F_{13}$ | Rod displacement sensor fault | [-1, 1] |
| | $F_{14}$ | Pressure sensor fault | [-1, 1] |
| | $F_{15}$ | Positioner spring fault | [0, 1] |
| External faults | $F_{16}$ | Positioner supply pressure fault | [0, 1] |
| | $F_{17}$ | Unexpected pressure change in valve | [-1, 1] |
| | $F_{18}$ | Fully or partly opened bypass valves | [0, 1] |
| | $F_{19}$ | Flow rate sensor fault | [-1, 1] |

vides information about the magnitudes of faults that can be simulated in the DAMADICS model. The magnitudes are categorized as small for values ranging from 5% to 35%, medium for values between 35% and 70%, and big for values between 70% and 100% in the case of abrupt faults. Incipient faults, on the other hand, gradually increase their magnitude over time. Detecting incipient faults at an early stage can be challenging, especially when the measured signals are noisy [47].

Table 3: Faults without physical interpretation.

| Fault | Small | Medium | Big | Incipient |
|---|---|---|---|---|
| $F_1$ | | | | ☒ |
| $F_3$ | | ☒ | ☒ | |
| $F_4$ | ☒ | ☒ | ☒ | |
| $F_8$ | | | | ☒ |
| $F_{11}$ | ☒ | ☒ | | |

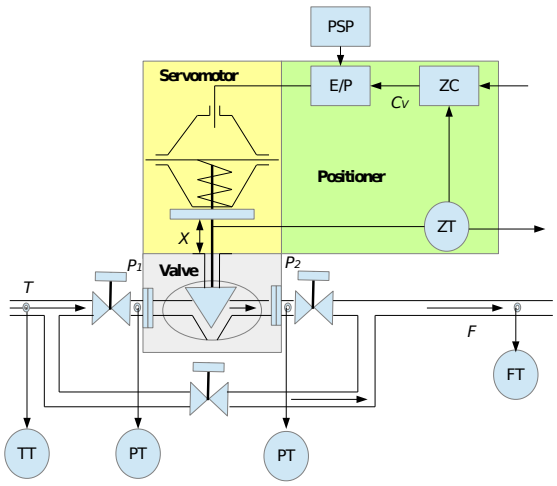


Figure 1: Scheme of DAMADICS actuator.

The DAMADICS actuator is depicted in Figure 1, where the three main components are distinguished by different colors. The diagram showcases the input and output variables associated with the system. The yellow-highlighted component represents the spring-and-diaphragm pneumatic servomotor, which facilitates the interaction between the control signal and the final movement. To better understand the nomenclature used in Figure 1, please refer to Table 4.

The DAMADICS model was implemented using Simulink®, a popular simulation software. To ensure accurate simulation results, certain considerations were taken into account. The ordinary differential equations (ODEs) describing the system dynamics were solved using the fourth-order Runge-Kutta method (ode4) with a fixed step size of 0.0025 seconds. This choice of solver and step size helps ensure numerical stability and accuracy in the simulation.

In addition, it is important to note that the output of the simulated process is subject to noise, which reflects the realistic conditions of industrial systems. All inputs and outputs in the model have band-limited white noise superimposed with a 50 Hz sine wave. The sine bias is set to 2.5% of disturbed signal nominal range and its amplitude is 2.5% of signal nominal range [20]. The presence of noise in the output signals adds a level of complexity to the fault detection and isolation process, as it introduces uncertainty and can affect the accuracy of the results.

Moreover, some specific faults in the DAMADICS model are characterized by a parameter $t_{fd}$, which repre-

Table 4: Faults in the DAMADICS model.

| Nomenclature | Description |
|---|---|
| E/P | Electro-pneumatic transducer |
| FT | Flow rate transmitter |
| PSP | Positioner supply pressure unit |
| PT | Pressure transmitter |
| TT | Temperature transmitter |
| ZC | Internal position controller |
| ZT | Stem position transmitter |

sents the fault development time. This parameter is particularly relevant for simulating incipient faults, which gradually increase in magnitude over time. By incorporating the fault development time parameter, the model can accurately capture the behavior of such incipient faults and their impact on the system dynamics.

Lastly, it is worth mentioning that the sampling time for collecting data from the simulated system is set to 1 second. This choice of sampling time aligns with the sampling rate typically used in the supervisory control and data acquisition (SCADA) systems deployed in real-world industrial environments, such as the sugar factory in Lublin.

These considerations ensure that the DAMADICS model accurately represents the behavior of the physical system and provides a realistic foundation for conducting fault detection and isolation experiments.

# 3 Methodology used for fault detection and isolation

In the field of fault detection and isolation (FDI), [48] employed an inverse fuzzy model for fault reconstruction. Given the Tennessee Eastman process, which offers numerous state variables for measurement [14, 49], the methodology adopted least angle regression for variable selection [50]. The faults were encoded in terms of amplitude and effectively isolated. However, it should be noted that in certain cases, the FDI process required a minimum of 1000 sample times. Additionally, other FDI techniques have been explored, such as partial least squares [51], elastic net [52], and least absolute shrinkage and selection operator algorithm [53].

## 3.1 Fuzzy modeling

In order to establish a fuzzy model, it is essential to define the discourse universe of the variables, which determines the fuzzy partition [54]. The ranges of the variables were presented by [9] in its Table 1, and the specific values utilized in this study are summarized in Table 5.

The inversion of the fuzzy model requires a monotonic model [31]. In a study by [55], a fuzzy model of a greenhouse was developed using two membership functions to ensure a monotonic model. The control is achieved by inverting the fuzzy model. In this context, two membership functions are constructed for the fuzzy partition of variables $C_V$, $P_1$, $P_2$, and $f$, while variable $T$ remains constant throughout the simulation. As a result, the fuzzy model aims to approximate variables $X$ and $F$.

Table 5: Ranges and units of the variables.

| Variable | Range |
|---|---|
| $C_V$ | 0–100% |
| $P_1$ | 0–4000 KPa |
| $P_2$ | 0–4000 KPa |
| $T$ | 0–200°C |
| $X$ | 0–100% |
| $F$ | 0–40 $m^3$/h |

The fuzzy rules can be denoted as [56]:

$$\begin{aligned} \text{If:} \quad & C_V(k) \text{ is } \tilde{A} \text{ and } P_1(k) \text{ is } \tilde{B} \text{ and } P_2(k) \\ & \text{is } \tilde{C} \text{ and } f(k) \text{ is } \tilde{D} \text{ and } X(k) \text{ is } \tilde{E} \ldots \\ & \text{and } F(k) \text{ is } \tilde{F}, \\ \text{then:} \quad & X_{apr}(k+1) = \theta, \end{aligned} \tag{1}$$

where $k$ is the sample, $\tilde{A}$ is a fuzzy set, and the rule consequent is $\theta$.

The fuzzy value obtained for each variable using a fuzzy set is denoted for example as $\mu_{\tilde{A}_1}(C_V(k))$.

The rule evaluation is:

$$\begin{aligned} \lambda_1(k) &= \mu_{\tilde{A}_1}(C_V(k))\mu_{\tilde{B}_1}(P_1(k))\mu_{\tilde{C}_1}(P_2(k)) \\ &\quad \mu_{\tilde{D}_1}(f(k))\mu_{\tilde{E}_1}(X(k))\mu_{\tilde{F}_1}(F(k)), \end{aligned} \tag{2}$$

$$\begin{aligned} \lambda_2(k) &= \mu_{\tilde{A}_1}(C_V(k))\mu_{\tilde{B}_1}(P_1(k))\mu_{\tilde{C}_1}(P_2(k)) \\ &\quad \mu_{\tilde{D}_1}(f(k))\mu_{\tilde{E}_1}(X(k))\mu_{\tilde{F}_2}(F(k)), \end{aligned}$$

and so on until to compute $\lambda_{64}(k)$.

The fuzzy partition for each variable is created by employing two membership functions. These functions utilize two limits to achieve a membership value of one. A line connects the maximum value to the zero value, which is positioned below the other limit. This construction ensures that the sum of membership values is always equals to one, thereby guaranteeing the monotonic nature of the fuzzy model [55].

There are a total of 64 fuzzy rules, because each one of the six variables is partitioned into two fuzzy sets. The membership values are arranged in a specific order to invert the fuzzy model. For this reason, the membership values assigned to the rules using $\mu_{\tilde{D}_1}(f(k))$ and $\mu_{\tilde{D}_2}(f(k))$ for the fuzzy partition of the fault $f(k)$ are placed in the last two columns of $\beta$. This arrangement results in a matrix $\beta \in \mathbb{R}^{n\times 64}$, which is utilized for the inversion of the fuzzy model. Here, $n$ represents the number of samples used for constructing the fuzzy model.

A normalization factor, denoted as $\Gamma_{i,j}$, can be computed when the summation of membership values does not equal one. It is calculated as $\Gamma_{i,j} = \beta_{i,j} / \sum_{j=1}^{2} \beta(i,j)$. The

least squares method is employed to compute the rule consequents $\theta$ using the normalized values in $\Gamma$. It is worth noting that the temperature variable $T$ was not included in the fuzzy model as it does not appear to be sensitive to faults.

Some fault types can be simulated in each case, and only the ones with a physical interpretation were used for modeling. Finally, $\theta$ is computed by using:

$$\theta_F = (\Gamma^T\Gamma)\Gamma^T F_+, \tag{3}$$

where $F_+$ represents the measure taken with an advance of one sample, i.e. the model must obtain the system behavior for the next sample. Thus, the fuzzy model obtains $F_{fuzzy} = \Gamma\theta_F$. A fuzzy model can be obtained in the same way to approach $X(k+1)$. In that case, the consequents of the rules are in $\theta_X$

Since the fuzzy model estimates two output variables, two sets of consequents are obtained: $\theta_F$ for approximating the flow rate $F$, and $\theta_X$ for the displacement of the valve head.

In some cases, the model obtained using $\theta_F$ closely approximates the actual variable $F$. In order to reconstruct a fault, it is necessary for the fault signal to cause a change in the output variables $F$ or $X$. Moreover, if this change is proportional to the magnitude of the fault, the fault signal can be reconstructed. For instance, in Fig. 2, the fuzzy model obtained to approximate $F$ when fault $F_1$ occurs at different magnitudes over time is shown. The corresponding fault signal is also depicted, illustrating a noticeable modification in the flow rate behavior. Similarly, in Fig. 3, the same situation is demonstrated. In this case, the fault $F_{17}$ is simulated, including the incipient case. It can be observed that the change in $F$ exhibits similar behavior for different fault magnitudes.

As mentioned above, a sampling time of one second is used, and the process inputs are normalized sinusoidal signals. This choice allows for modifications in the operating conditions and the inclusion of nonstationary signals. By using signals with different frequencies and amplitudes, the model can capture various dynamics and better represent real-world scenarios.

The inputs are defined as:

$$C_V(k) = 0.5 + 0.25\sin(0.01k), \tag{4}$$
$$P_1(k) = 3500,000 + 175,000\sin(0.1k), \tag{5}$$
$$P_2(k) = 2600,000 + 26,000\sin(k/\pi). \tag{6}$$

The temperature is assumed constant $T = 43°C$ [57]. All the variables are noisy, and the pressure measures are the disturbed values obtained from the model.

## 3.2 Fuzzy model inversion

To invert the fuzzy model, the process variables are evaluated independently of the fault signal $f(k)$. This results in obtaining 32 rules for the inversion process. The consequents, represented by $\theta_F$ in this case, are organized into two columns. The values in one column correspond to the consequents obtained using the first limit $\tilde{D}_1$ for $f$, while the values in the other column correspond to the consequents obtained using the second limit $\tilde{D}_2$, as shown in Equation (1). These two columns are combined to form the matrix $\Theta \in \mathbb{R}^{32\times 2}$, which contains the consequent parameters for the inversion process.

The first step in the fault reconstruction process is to calculate the first center of the fuzzy partition. This is done by multiplying the 32 membership values $\mu(k)$ with the values in the first column of $\Theta$ using the Hadamard product. Similarly, the second limit $\tilde{F}_2^*$ is obtained by multiplying the membership values with the values in the second column of $\Theta$, following a similar procedure as Equation (1) shows.

To obtain the membership values for the original signal $F(k)$ using the new fuzzy sets, the signal is evaluated by the new fuzzy sets. These new membership values are then multiplied with the limits used to fuzzify $f$, which are

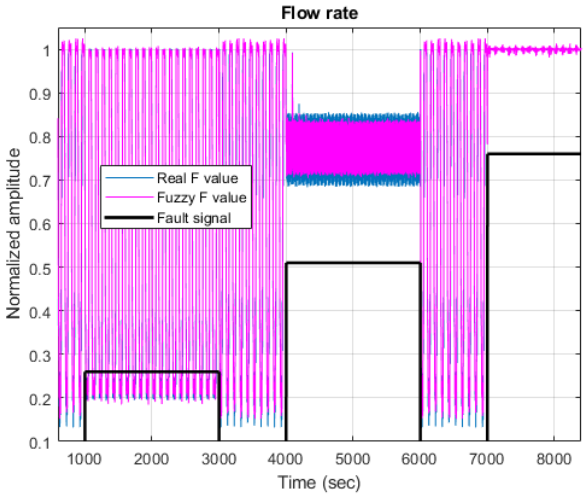


Figure 2: Comparison between flow rate $F$ and its fuzzy approximation under fault $F_1$.

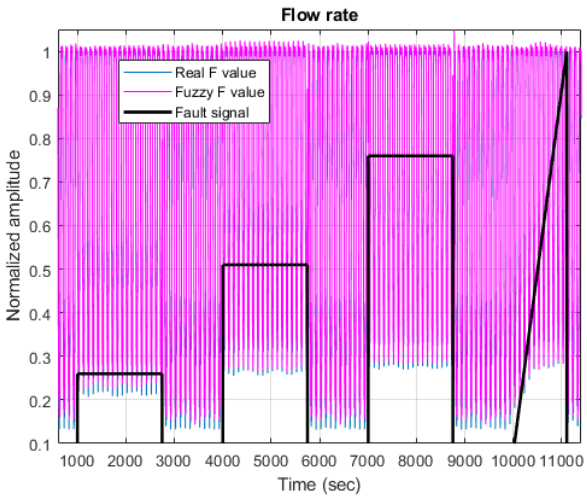


Figure 3: Comparison between flow rate $F$ and its fuzzy approximation under fault $F_{17}$.

$[\tilde{D}_1 \ \tilde{D}2]^T$. This process yields two values, which are used to approximate the reconstructed fault signal $fapr$.

Similarly, if we want to invert the fuzzy model used to approach $X$, the new limits $[\tilde{E}_1^* \ \tilde{E}_2^*]$ to fuzzify $X$ are obtained, and the fault reconstruction is:

$$f_{apr}(k) = [\mu_{\tilde{E}_1^*}(X(k)) \ \mu_{\tilde{E}_2^*}(X(k))] \ [\tilde{D}_1 \ \tilde{D}_2]^T. \quad (7)$$

The fuzzy model inversion can be briefly explained following the next steps:

1. The consequents $\theta$ of the 64 fuzzy rules are ordered to form $\Theta$ that has as first column the 32 membership values corresponding for the case when the rules evaluated use the first fuzzy set for the partition of fault $f(k)$, i.e. $\tilde{D}_1$. The second column correspond to the 32 rules that contains the membership values when fuzzy set $\tilde{D}_2$ was used.

2. The current variables values are evaluated by their respective fuzzy sets, i.e. we obtain $\mu_{\tilde{A}_1}(C_v(k))$, $\mu_{\tilde{A}_2}(C_v(k))$, $\mu_{\tilde{B}_1}(P_1(k))$, …, $\mu_{\tilde{F}_2}(F(k))$.

3. Now all this membership valued are use to evaluate a fuzzy rule, the product was used in this step, i.e.

$$\begin{aligned} R_1(k) &= \mu_{\tilde{A}_1}(C_v(k))\mu_{\tilde{B}_1}(P_1(k))\mu_{\tilde{C}_1}(P_2(k)) \\ &\quad \cdots \mu_{\tilde{F}_1}(F(k)) \\ R_2(k) &= \mu_{\tilde{A}_1}(C_v(k))\mu_{\tilde{B}_1}(P_1(k))\mu_{\tilde{C}_1}(P_2(k)) \\ &\quad \cdots \mu_{\tilde{F}_2}(F(k)) \end{aligned}$$

until,

$$\begin{aligned} R_{32}(k) &= \mu_{\tilde{A}_2}(C_v(k))\mu_{\tilde{B}_2}(P_1(k))\mu_{\tilde{C}_2}(P_2(k)) \\ &\quad \cdots \mu_{\tilde{F}_2}(F(k)) \end{aligned}$$

4. The new centers $\tilde{E}_1^*$ and $\tilde{E}_2^*$ if the fuzzy model for $X$ is inverted, or $\tilde{F}_1^*$ and $\tilde{F}_2^*$, are computed multiplying the evaluation rules of step 3 and the matrix $\Theta$.

5. The model inversion use the fuzzy model of $X$ or $F$, to obtain the fault $f$. Then, the signal used, e.g. $F$ is evaluated by the new fuzzy sets with centers $\tilde{F}_1^*$ and $\tilde{F}_2^*$.

6. Finally, the fault approach is obtained by multiplying these last membership values and the centers used initially for the fuzzy partition of fault signal $\tilde{D}_1$ and $\tilde{D}_2$.

To illustrate this procedure Fig. 4 shows how to obtain the new centers used to obtain the fault than generates the current signals behavior.

The fault reconstruction, as depicted in Fig. 5, appears to be noisy and may not immediately reveal the presence of the fault signal. However, we applied a filtering technique to the reconstructed signal, and the fault signal becomes more discernible. In this case, a second-order low-pass filter with

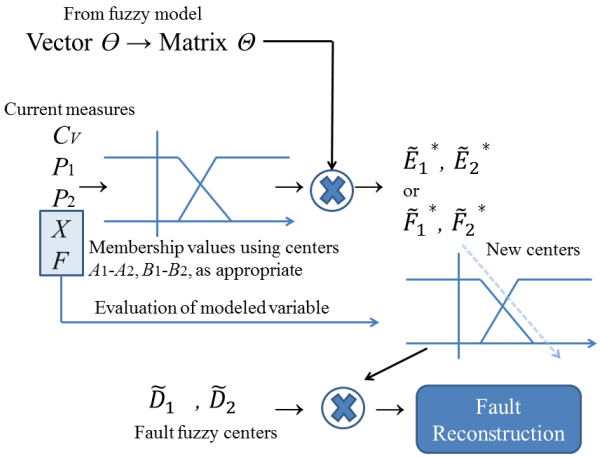


Figure 4: Fuzzy model inversion.

two poles at $-0.01$ is proposed. This filter has a lower frequency of 0.01 and provides an attenuation of $-40dB$ per decade.

To implement the filter in a discrete system, a zero-order hold discretization method is utilized [58]. The resulting filter in the Z transform domain is given by the following equation:

$$\frac{f_{filt}(z)}{f_{apr}(z)} = \frac{4.967e-8z+4.934e-5}{z^2-1.98z+0.9802}.$$

due to filtering, a delay is obtained. However, the fault takes some samples to be detected, also when a fault disappears (an intermittent fault), the systems takes some seconds to recover its normal performance.

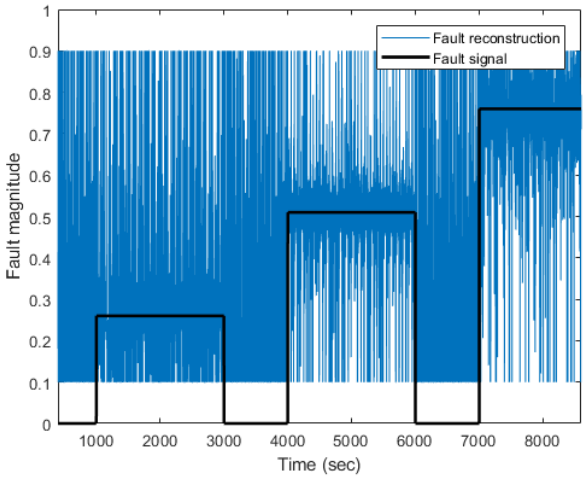


Figure 5: $F_{apr}$ by inverting the fuzzy model of $F$.

The filtered fault reconstructions obtained by inverting the fuzzy models for fault $F_6$ and fault $F_{17}$ are illustrated in Fig. 6 and Fig. 7, respectively. In Fig. 6, specific thresholds are depicted, which can be utilized for the detection

and classification of fault $F_6$.

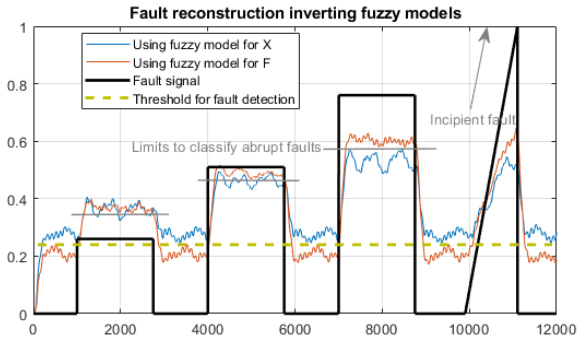


Figure 6: $F_6$ reconstruction by inverting both fuzzy models.

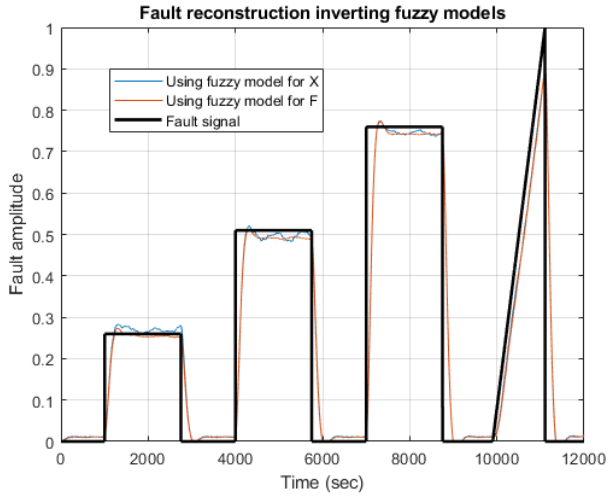


Figure 7: $F_{17}$ reconstruction by inverting both fuzzy models.

In the majority of cases, the fuzzy model for the flow rate $F$ yields the most accurate and reliable fault reconstruction. However, when attempting to reconstruct faults $F_8$ and $F_{15}$ specifically, the model for the displacement $X$ provides superior results. It is worth noting that if a fault does not manifest itself clearly in the process outputs, it becomes challenging to accurately reconstruct such faults.

Due to the presence of noise in the signals, a threshold-based approach can be employed to detect faults. This involves using the average value of the fault-free signal $f_{filt}$, along with twice the standard deviation within that specific period, as a reference threshold. It is important to note that the system being analyzed is nonlinear, meaning that the response to a fault may not be directly proportional to the fault magnitude. Consequently, the reconstructed fault values may exhibit different magnitudes compared to the actual faults.

For fault classification purposes, different thresholds can be utilized. In the case of incipient faults, their behavior typically intensifies over time. As such, an alternative approach involves assessing whether the current fault reconstruction demonstrates continuous changes with the same sign. However, due to the presence of noise, the signal $f_{filt}$ tends to fluctuate. Therefore, it is necessary to analyze at least four samples to ensure that the signal consistently exhibits either an increasing or decreasing trend.

Fault isolation is achieved by comparing the responses of different fuzzy models to the current signals obtained. Since each fuzzy model was built for a specific case, the model that yields the highest response (membership value) is used for fault isolation.

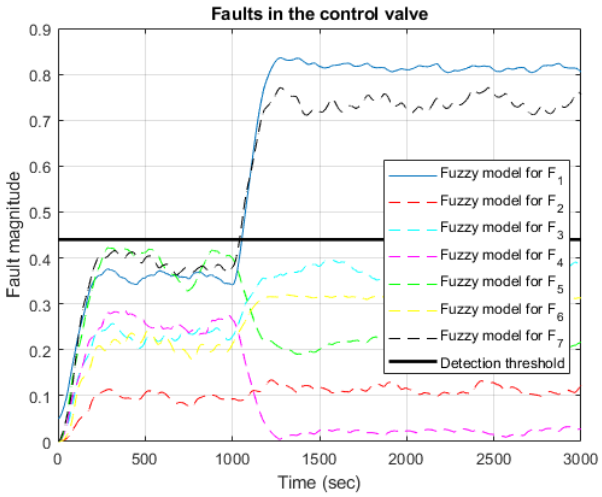


Figure 8: $F_1$ evaluated by different fuzzy models.

Figure 8 illustrates the fault reconstruction using the fuzzy models for faults $F_1, F_2, \ldots, F_7$, which are associated with faults in the control valve. It is evident that these faults can be detected. However, for fault isolation, it is necessary to evaluate the response of the inverse fuzzy models. Four fuzzy systems are employed for fault isolation. The first fuzzy system evaluates faults $F_1, F_2, \ldots, F_7$ related to the control valve, while the second fuzzy system considers faults $F_8, F_9, \ldots, F_{11}$ in the servomotor. The third fuzzy system incorporates $F_{12}, F_{13}, \ldots, F_{15}$ to describe faults in the positioner. Lastly, the fourth fuzzy system utilizes $F_{16}, F_{17}, \ldots, F_{19}$ for external faults (refer to Table 2).

The FDI proposal involves constructing a fuzzy model to approximate the output signals of the DAMADICS model. By inverting these fuzzy models, the fault signal can be reconstructed using the currently measured signals. Once fault detection is performed, the reconstructed signals are categorized into four sets, corresponding to each fault source: control valve, servomotor, positioner, and external faults. These grouped signals are then inputted into a fuzzy system for fault isolation. The schematic diagram illustrating this technique is presented in Figure 9.

It is worth mentioning that the use of an unknown input observer for fault reconstruction with $H_\infty$ performance has been explored in [59]. Additionally, [60] proposed an intriguing approach that involves inverting certain filters to detect faults in a nonlinear system. This approach shares

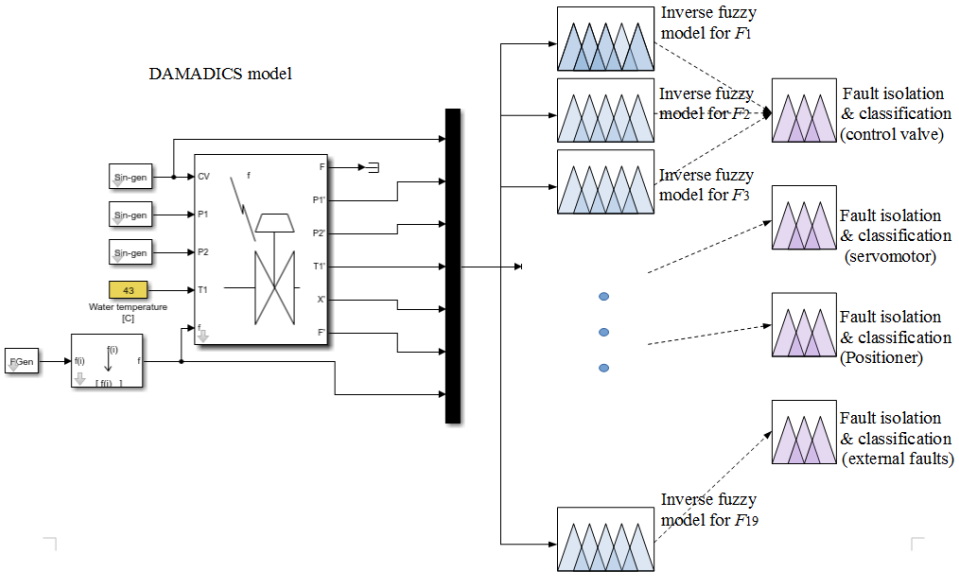


Figure 9: Fault detection and isolation scheme.

similarities with the current application, as a fuzzy system can be considered as a type of nonlinear filter.

Similarly, Varkonyi [61] used a genetic algorithm for iterative fuzzy model inversion. His approach involves interchanging one of the inputs with the output in order to invert the fuzzy model. The genetic algorithm was employed to optimize the model inversion process.

By adopting this approach, the fuzzy model can be effectively inverted, enabling the estimation or reconstruction of the input variable based on the observed output. This iterative process using a genetic algorithm allows for the refinement and improvement of the model inversion, leading to more accurate results.

In contrast, [62] employed the system's model to design sliding mode observers. They utilized individual state estimators based on least squares to enable rapid fault reconstruction for FDI applications. This approach differs from the fuzzy model-based technique described earlier.

## 3.3 Wavelet transform to highlight faults

Wavelets are a powerful tool in signal processing that can effectively detect abrupt changes in signals caused by faults in a system. Unlike stationary events, faults are nonstationary, making wavelets particularly well-suited for fault detection. Wavelet functions are derived from translating (mother wavelet) and scaling (father wavelet) functions to create an orthonormal basis [63]. This allows wavelets to capture both time and frequency information simultaneously, making them ideal for analyzing signals with transient behavior.

The wavelet transform can be utilized to emphasize the existence of a fault within a signal [48]. In the case of discrete wavelet transform, a sufficient number of samples is required for signal decomposition. For instance, if an eighth decomposition level is desired, a minimum of $2^8 = 256$ samples is needed to obtain a meaningful indication of a fault. However, for online fault diagnosis, it is advisable to employ the continuous wavelet transform, where only the selection of the mother wavelet and the scale is necessary [64]. This approach allows for real-time fault detection and characterization without the need for a predefined number of samples or decomposition levels.

The scalogram of the signal $X$ when fault $F_1$ is depicted in Fig. 10. In order to determine the appropriate scale, the row where all fault occurrences are clearly visible is chosen. Subsequently, the continuous wavelet transform is employed as a filtering technique to localize transients. The wavelet transform plot is shown in Fig. 11. This analysis provides a visual representation of the signal characteristics and highlights the presence of fault-related features.

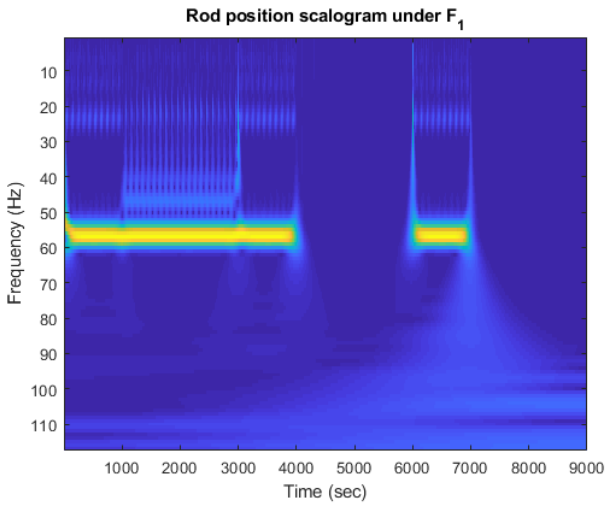


Figure 10: Scalogram to select frequency.

The wavelet transform is particularly effective for detect-

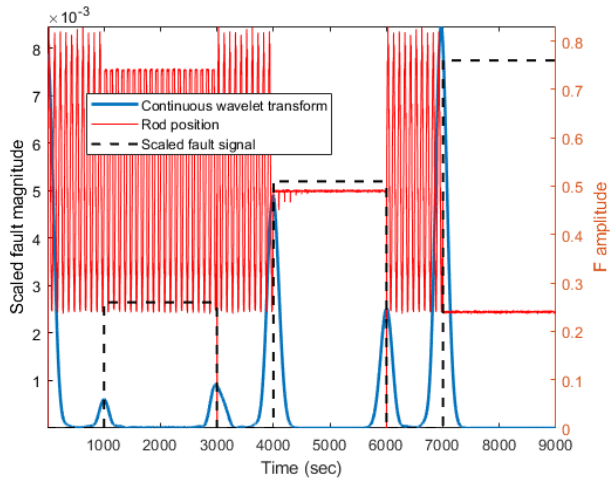


Figure 11: Wavelet transform to localize transients.

ing nonstationary fault signals [65]. It can identify changes in the measurement data that indicate the presence or absence of an event [66]. Therefore, the wavelet transform enables the detection of faults as they occur and as they cease. However, selecting an appropriate scale for fault detection can pose a challenge. It is crucial to consider that the fault may not manifest until at least 200 samples after the simulation or system operation begins, while detection of the fault can occur as early as 50 samples into the process due to the chosen scale of the wavelet.

To streamline the computation of the wavelet transform, a line-based approach is employed instead of shifting the wavelet along the signal being analyzed. This approach involves maintaining a vector that contains the wavelet evaluations, and performing convolutions with the incoming samples. By examining the amplitude of the wavelet transform at the designated scale for each fault, fault classification can be achieved, as demonstrated in Fig. 11. However, fault isolation requires the utilization of the inverse fuzzy model.

The specific wavelet employed for detecting fault levels that are imperceptible to the fuzzy model is the analytic Morlet wavelet. This wavelet is commonly used for edge detection in image processing [67]. The equation representing the wavelet function is as follows:

$$\Psi(t) = e^{-\alpha t^2} e^{2\pi f_c t \mathrm{i}}, \tag{8}$$

where the center frequency is $f_c$ and the width of the Gaussian function is $\alpha$.

Using (8), the wavelet transform is:

$$W_\Psi f(a,b) = \frac{1}{\sqrt{a}} \int_{-\infty}^{\infty} f(t) \Psi^* \left( \frac{t-b}{a} \right) dt, \tag{9}$$

where $b$ is the time shift and $a$ is the scale selected regarding the scalogram. Due to the signal being sampled each second, the scale used to obtain Fig. 11 was 63, and then the wavelet function 8 is scaled, shifted, and discretized, then the convolution with the signal $X$ was made to detect transients.

To classify faults such as $F_8$, $F_9$, $F_{11}$, $F_{14}$, and in some cases $F_1$, $F_{12}$, and $F_{16}$, the wavelet transform is employed to filter the output signals and identify the fault severity. However, it should be noted that wavelets are primarily useful for fault detection [68]. An interesting approach was proposed in [63], where the Daubechies wavelet was utilized to detect faults in the DAMADICS actuator, with a requirement for fault detection within 15 seconds.

# 4 Results

The simulation incorporates various magnitudes for the fault signals. Magnitudes of 25%, 50%, and 75% were utilized to represent small, medium, and large abrupt faults, respectively. In the case of incipient faults, the magnitude increases gradually from zero to 100% over a duration of 1200 seconds. To classify a fault as incipient, a minimum of four samples is required to assess if the fault exhibits a continuous change over time.

Considering the aforementioned information, it is important to note that the results obtained for fault detection and classification may not be fully representative in certain cases. Furthermore, the detection and isolation of faults often require a specific fault magnitude to be present.

The simulations were conducted by evaluating the downloaded model in MATLAB® R2017b on a laptop equipped with an Intel® Core$^{TM}$ i5-4200U processor running at 2.3 GHz, and with 4 GB of RAM.

## 4.1 Fault detection

Fault detection refers to the ability to recognize the occurrence of a fault. In this study, an inverse fuzzy model was developed for each individual fault, resulting in a total of 19 fuzzy models. Among these models, the one that provides the best approximation to the behavior of the variable $X$ is selected as the optimal choice. To streamline computational efforts, only one model is utilized for the detection of each specific fault.

Fault detection is accomplished by applying a threshold to the fault reconstruction signal. Due to the presence of nonlinearities, the filtered fault signal ($f_{filt}$) deviates from zero even in the absence of any simulated fault. Consequently, the threshold is computed by determining the average value of $f_{filt}$ when the fault signal is equal to zero, and then adding double the standard deviation for this condition.

The fault detection rate (FDR) serves as an evaluation metric to assess the effectiveness of the proposed technique. FDR represents the percentage of correctly identified faulty values when $f_{filt}$ exceeds a specified threshold (also known as true positives). It is worth noting that many studies employ datasets containing both faulty and fault-free signals. However, when the fault is no longer

present, it may take several samples for the system to return to its normal behavior. This circumstance can lead to an increased number of false alarms. In this work, such cases are also considered and taken into account during the evaluation process.

The evaluation of fault detection performance involves the use of various metrics. These metrics utilize the following terms: true positive ($tp$), which denotes the correct detection of a sample fault; true negative ($tn$), which represents the accurate identification of a fault-free signal as normal system behavior; false positive ($fp$), which refers to the erroneous detection of normal operation data as faulty (false alarm); and false negative ($fn$), which indicates the misclassification of fault measures as normal system operation. Several characteristics are employed to assess the performance of fault detection and isolation (FDI), including the following metrics [69]:

$$\text{Precision} = \frac{tp}{tp+fp}, \tag{10}$$

$$\text{Memory} = \frac{tp}{tp+fn}, \tag{11}$$

$$\text{Specificity} = \frac{tn}{tn+fp}, \tag{12}$$

$$\text{Accuracy} = \frac{tp+tn}{tp+fp+tn+fn}. \tag{13}$$

Table 6 presents the metrics used to evaluate the fault detection performance of the inverted fuzzy models. When the value in the first column is less than 0.5, it indicates that there are more false alarms than actual fault detections. A memory value below 0.5 implies that the algorithm fails to detect a significant portion of the faulty data. A specificity value lower than 0.5 suggests that the false alarms outnumber the instances of normal behavior without faults. The accuracy parameter is particularly significant as it determines whether real faults were successfully detected, with the algorithm assuming normal operation in the absence of faults.

## 4.2 Fault isolation

Fault isolation refers to the ability to differentiate between different faults occurring in a process. During the simulation, we observed that certain faults need to reach a certain magnitude to be detected, as their effects may be imperceptible in the measured signals from the DAMADICS model. The fault reconstruction process aids in estimating the magnitude of the fault responsible for the current behavior in the system. Consequently, fault isolation and classification are achieved simultaneously. However, in a different application discussed by [8], a fuzzy classifier was required to classify different fault magnitudes for the same fault type.

In this study, a total of 19 fuzzy models were employed. For fault detection, isolation, and classification, a fuzzy model was specifically developed to approximate the behavior of $X$ when simulating faults $F_8$ and $F_{15}$ due to the superior results obtained, characterized by fewer false alarms and a higher detection rate. For the remaining faults, we use the fuzzy models focused on approximating the behavior of $F$.

For fault isolation, it was necessary to establish certain threshold values for fault magnitudes: $F_1 > 31\%$, $F_7 > 41.5\%$, $F_{12} > 42\%$, and $F_{16} > 60\%$. If these conditions were met, fault isolation was found to be 98% accurate in all cases. Additionally, the fault detection characteristics presented in Table 6 exhibited higher values. Simulations were conducted for fault types that have a physical interpretation. Table 7 displays the obtained fault classifications, where fault isolation was determined by comparing the values of $f_{filt}$, with the larger value indicating the fault present in the system.

The symbol ☒ indicates that the fault was not simulated due to its physical background [57], × denotes that the fault type could not be classified, and ✓ signifies a correct classification. Faults that could not be classified were attributed to $f_{filt}$ exhibiting similar magnitudes regardless of the fault magnitude. Fortunately, the faults were accurately isolated when the fault magnitudes for $F_1$, $F_7$, $F_{12}$, and $F_{16}$ were as previously mentioned.

If the fault magnitude does not reach a certain threshold for detection, it is not considered in the analysis. The fault detection characteristics presented in Table 6 can be summarized as follows in Table 8.

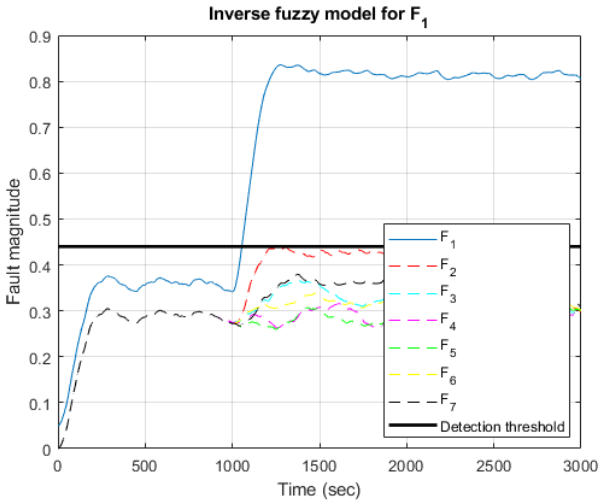


Figure 12: Inverse fuzzy model for $F_1$ evaluated with different faults.

Similarly to what is shown in Fig. 8 for the simulation and fault reconstruction using different inverse fuzzy models, the fault isolation results are presented in Fig. 12.

To evaluate the performance of fault isolation, a confusion matrix is utilized, as commonly done in fault diagnosis studies [70]. The confusion matrix reflects the accuracy of fault isolation, with higher values along the diagonal indicating successful isolation. In Fig. 13, it can be observed that faults $F_8$, $F_9$, $F_{13}$, $F_{14}$, and $F_{17}$ pose greater challenges for isolation, despite exhibiting a good detection rate.

Table 6: Fault detection in the DAMADICS model.

| Fault origin | Fault | Precision | Memory | Specificity | Accuracy |
|---|---|---|---|---|---|
| Control valve | $F_1$ | 0.9521 | 0.6541 | 0.9344 | 0.7496 |
| | $F_2$ | 0.8824 | 0.9724 | 0.8524 | 0.9163 |
| | $F_3$ | 0.8596 | 0.8610 | 0.9078 | 0.8901 |
| | $F_4$ | 0.5367 | 0.6908 | 0.8950 | 0.8644 |
| | $F_5$ | 0.9258 | 0.8176 | 0.9249 | 0.8669 |
| | $F_6$ | 0.9067 | 0.9759 | 0.8835 | 0.9331 |
| | $F_7$ | 0.9265 | 0.6856 | 0.9359 | 0.8005 |
| Servomotor | $F_8$ | 0.7224 | 0.1786 | 0.9094 | 0.4778 |
| | $F_9$ | 0.9086 | 0.1304 | 0.9859 | 0.5215 |
| | $F_{10}$ | 0.8116 | 0.8389 | 0.7741 | 0.8089 |
| | $F_{11}$ | 0.9159 | 0.5841 | 0.9482 | 0.7693 |
| Positioner | $F_{12}$ | 0.9038 | 0.5994 | 0.9260 | 0.7507 |
| | $F_{13}$ | 0.9003 | 0.9818 | 0.8738 | 0.9318 |
| | $F_{14}$ | 0.2342 | 0.0312 | 0.8866 | 0.4121 |
| | $F_{15}$ | 0.8471 | 0.9778 | 0.7952 | 0.8932 |
| External faults | $F_{16}$ | 0.7372 | 0.4718 | 0.8049 | 0.6260 |
| | $F_{17}$ | 0.8695 | 0.9964 | 0.8265 | 0.9177 |
| | $F_{18}$ | 0.9065 | 0.9659 | 0.8832 | 0.9282 |
| | $F_{19}$ | 0.8830 | 0.9908 | 0.8477 | 0.9246 |

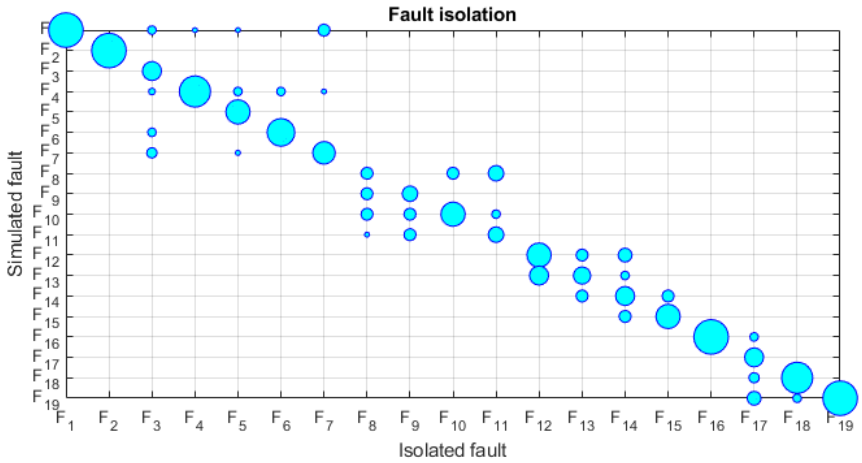


Figure 13: Confusion matrix.

# 5 Discussion

The obtained fault detection rates are consistent with those reported in the literature. However, the use of inverse fuzzy models contributes significantly to fault isolation, which is not extensively addressed in existing papers focusing on the DAMADICS model. These models provide a means to classify faults based on their magnitude and behavior, enabling comprehensive fault diagnosis. One limitation is the reliance on the model that yields the highest response to ensure accurate fault isolation.

## 5.1 Comparison of detection rates

The fault detection rate obtained in this study is 84.81%, which significantly outperforms the rates reported in other works, such as 55.45% and 82.37%. This improvement can be attributed to the use of inverse fuzzy models combined with wavelet transform, which enhances the detection of small and abrupt faults that are often missed by conventional methods. Our method demonstrates higher sensitivity and reliability in identifying faults, thereby reducing the risk of undetected issues in chemical processes. A comparison of the obtained results for fault detection is presented in Table 9, alongside the results from [37] and [43]. The best results are highlighted in bold.

## 5.2 Analysis of computational efficiency

Our approach also shows advantages in terms of computational efficiency. The inversion of fuzzy models is computationally less intensive compared to other advanced tech-

Table 7: Fault classification in the DAMADICS model.

| Fault origin | Fault | Small | Medium | Big | Incipient |
|---|---|---|---|---|---|
| Control valve | $F_1$ | × | ✓ | ✓ | ⊞ |
| | $F_2$ | ✓ | ✓ | ✓ | ✓ |
| | $F_3$ | ⊞ | ⊞ | ⊞ | ✓ |
| | $F_4$ | ⊞ | ⊞ | ⊞ | ✓ |
| | $F_5$ | ✓ | ✓ | ✓ | ✓ |
| | $F_6$ | ✓ | ✓ | ✓ | ✓ |
| | $F_7$ | × | ✓ | ✓ | ✓ |
| Servomotor | $F_8$ | × | × | × | ⊞ |
| | $F_9$ | × | × | × | × |
| | $F_{10}$ | ✓ | ✓ | ✓ | ✓ |
| | $F_{11}$ | ⊞ | ⊞ | × | × |
| Positioner | $F_{12}$ | × | ✓ | ✓ | ✓ |
| | $F_{13}$ | ✓ | ✓ | ✓ | ✓ |
| | $F_{14}$ | × | × | × | × |
| | $F_{15}$ | ✓ | ✓ | ✓ | ✓ |
| External faults | $F_{16}$ | × | × | ✓ | ✓ |
| | $F_{17}$ | ✓ | ✓ | ✓ | ✓ |
| | $F_{18}$ | ✓ | ✓ | ✓ | ✓ |
| | $F_{19}$ | ✓ | ✓ | ✓ | ✓ |

Table 8: Fault detection for detectable levels in the DAMADICS model.

| Fault | Precision | Memory | Specificity | Accuracy |
|---|---|---|---|---|
| $F_1$ | 0.9521 | 0.9810 | 0.9606 | 0.9696 |
| $F_7$ | 0.9249 | 0.9797 | 0.9571 | 0.9650 |
| $F_{12}$ | 0.8705 | 0.8242 | 0.9341 | 0.8957 |
| $F_{16}$ | 0.8580 | 0.8532 | 0.9658 | 0.9439 |

niques like artificial neural networks or support vector machines. This efficiency is critical in real-time applications where prompt detection and isolation of faults are necessary to prevent process disruptions. The simplicity and lower computational requirements of our method make it suitable for integration into existing industrial systems without requiring significant hardware upgrades. A disadvantage is to require data to obtain the fuzzy models off-line before to use this proposal.

## 5.3 Robustness against noisy data and incipient faults

One of the key strengths of our approach is its robustness against noisy data and the detection of incipient faults. By employing wavelet transform, our method effectively filters out noise and enhances the signal corresponding to faults highlighting abnormal events. This robustness is crucial in real-world industrial environments where data is often contaminated with noise. Additionally, the capability to detect incipient faults allows for early intervention, preventing minor issues from escalating into major problems. Our method's superior fault isolation accuracy, at 78.85%, further underscores its effectiveness in distinguishing between different fault types, even in challenging conditions. For this reason a low-pass filter was needed to reconstruct the fault signals. However, the filter adds time to detect and isolate faults.

## 5.4 Improvement over state of the art techniques

Compared to state-of-the-art (SOTA) techniques, our method offers several improvements. While SOTA techniques like deep learning models provide high accuracy, they often require extensive computational resources and large datasets for training. In contrast, our inverse fuzzy model approach achieves competitive accuracy with lower computational demands and without the need for extensive data preprocessing. This balance of accuracy and efficiency makes our method a practical choice for fault detection in the chemical industry.

Among the faults considered, fault $F_9$ exhibits the lowest detection rate. To enhance the detection of this particular fault, alternative preprocessing methods can be explored instead of relying solely on the wavelet transform, as indicated by the results presented in Table 9. Notably, a detection rate exceeding 0.9 was achieved in the study by [43]. Grouping the fuzzy models based on the possible fault sources allows for a targeted comparison of models for fault isolation.

An intriguing avenue for future research involves developing fault-tolerant control strategies for the valve actuator under consideration, leveraging the insights gained from the fault diagnosis results.

Table 9: Fault detection rates comparison.

| Fault | This proposal | [37] | [43] |
|---|---|---|---|
| $F_1$ | 0.7480 | 0.031 | **0.9201** |
| $F_2$ | 0.9545 | **0.988** | 0.8333 |
| $F_3$ | **0.9592** | Not reported | 0.3663 |
| $F_4$ | **0.4451** | Not reported | Not reported |
| $F_5$ | **0.8275** | Not reported | 0.7228 |
| $F_6$ | **0.9761** | Not reported | 0.7327 |
| $F_7$ | 0.9265 | 0.988 | **1.000** |
| $F_8$ | 0.6952 | 0.121 | **0.9333** |
| $F_9$ | 0.5319 | Not reported | **0.9130** |
| $F_{10}$ | 0.8392 | 0.434 | **0.9167** |
| $F_{11}$ | 0.6308 | 0.409 | **0.8974** |
| $F_{12}$ | 0.6768 | 0.111 | **0.9302** |
| $F_{13}$ | **0.9823** | 0.880 | 0.0090 |
| $F_{14}$ | 0.4142 | Not reported | **0.8076** |
| $F_{15}$ | **0.9784** | 0.373 | 0.6863 |
| $F_{16}$ | 0.6221 | 0.094 | **0.8352** |
| $F_{17}$ | 0.9968 | **0.998** | 0.8393 |
| $F_{18}$ | **0.9818** | 0.834 | 0.9365 |
| $F_{19}$ | **0.9916** | 0.947 | 0.9716 |

In conclusion, our study demonstrates that the combination of inverse fuzzy models and wavelet transform provides a robust, efficient, and accurate method for fault detection, isolation, and classification. This approach not only enhances detection rates and computational efficiency but also offers superior robustness against noisy data and incipient faults, making it a valuable tool for maintaining the reliability and safety of chemical processes.

# 6 Conclusions

In this study, we demonstrate how inverse fuzzy models can be applied to fault reconstruction, facilitating the detection and isolation of faults. We utilized the DAMADICS benchmark, specifically focusing on the electro-pneumatic valve, as our case study for proposing and implementing fault diagnosis techniques. The effectiveness of the fuzzy models in fault detection was evident through the establishment of appropriate thresholds. However, due to the inherent noise present in the output signals, the inverse fuzzy models do not yield a zero output in the absence of faults. To address this issue, a filtering process was employed for fault reconstruction, albeit with the introduction of some delay.

Among the faults considered, $F_8$ and $F_{14}$ posed the greatest challenges in terms of detection. False alarms were observed with the inverse fuzzy models when simulating $F_{15}$ and $F_{16}$. However, for other fault types, the fault detection results were comparable to those reported in similar studies. Notably, improved results were achieved for faults $F_3 - F_6$, $F_{13}$, $F_{18}$, and $F_{19}$ compared to the literature. Nevertheless, in terms of fault isolation, the inverse fuzzy models exhibited similar behavior across different fault types, often leading to misinterpretation of certain faults such as $F_8$, $F_{13}$, $F_{14}$, and $F_{17}$ as other fault types.

When simulating faults $F_1$ or $F_7$, detection was possible, but classification proved challenging, particularly for small abrupt faults. Additionally, in the case of incipient faults, limitations arose due to the physical constraints, resulting in the simulation of only certain fault types. In these cases, a specific fault magnitude had to be applied for effective fault detection. Specifically, fault magnitudes greater than 31% for $F_1$, 41% for $F_7$, 42% for $F_{12}$, and 60% for $F_{15}$ were required. Notably, faults $F_8$, $F_9$, and $F_{14}$ could not be classified as small, medium, large, or incipient.

The use of wavelet transform proved beneficial in detecting small faults for $F_1$ and $F_7$. However, it did not contribute significantly to fault isolation. One limitation of the proposed methodology is the requirement of measured data during fault conditions to build fuzzy models for fault reconstruction. As future work, the integration of ANNs is planned to facilitate fault prognosis by identifying fault signatures. Additionally, the application of inverse fuzzy fault models holds promise for the development of fault-tolerant control strategies.

# Declaration of competing interest

The authors declare that they have no known competing financial interests or personal relationships that could have appeared to influence the work reported in this paper.

## Acknowledgement

The authors would like to thank the Mexican National Science and Technology Council, this paper was possible under grants of the National Laboratories program,

(LANAVEX, CONAHCyT).

# References

[1] M. Mansouri, M. Nounou, H. Nounou, and N. Karim, "Kernel PCA-based GLRT for nonlinear fault detection of chemical processes," *Journal of Loss Prevention in the Process Industries*, vol. 40, pp. 334–347, 2016. https://doi.org/10.1016/j.jlp.2016.01.011

[2] A. Imanaka, T. Murayama, S. Nishikizawa, and A. Nagaoka, "Local governments' response to accidents in chemical factories in Japan: Focus on petroleum industrial complexes special accident prevention areas," *International Journal of Disaster Risk Reduction*, vol. 74, p. 102880, 2022. https://doi.org/10.1016/j.ijdrr.2022.102880

[3] C. Chen and G. Reniers, "Chemical industry in China: The current status, safety problems, and pathways for future sustainable development," *Safety Science*, vol. 128, p. 104741, 2020. https://doi.org/10.1016/j.ssci.2020.104741

[4] J. N. P. Nogueira, P. A. Melo, and M. B. de Souza Jr., "Faulty scenarios in sour water treatment units: Simulation and AI-based diagnosis," *Process Safety and Environmental Protection*, vol. 165, pp. 716–727, 2022. https://doi.org/10.1016/j.psep.2022.07.043

[5] S. Bansal and J. T. Selvik, "Investigating the implementation of the safety-diagnosability principle to support defence-in-depth in the nuclear industry: A Fukushima Daiichi accident case study," *Engineering Failure Analysis*, vol. 123, p. 105315, 2021. https://doi.org/10.1016/j.engfailanal.2021.105315

[6] A. S. Yeardley, J. O. Ejeh, L. Allen, S. F. Brown, and J. Cordiner, "Integrating machine learning techniques into optimal maintenance scheduling," *Computers & Chemical Engineering*, vol. 166, p. 107958, 2022. https://doi.org/10.1016/j.compchemeng.2022.107958

[7] R. Doraiswami and L. Cheded, *Fault Diagnosis and Detection*, ch. Fault detection and isolation, pp. 1–27. IntechOpen, 2017. https://doi.org/10.5772/67870

[8] C. D. Bocaniala and J. S. da Costa, "Application of a novel fuzzy classifier to fault detection and isolation of the DAMADICS benchmark problem," *Control Engineering Practice*, vol. 14, pp. 653–669, 2006. https://doi.org/10.1016/j.conengprac.2005.06.008

[9] N. Hadroug, A. Hafaifa, and A. Daoudi, "Valve actuator fault classification based on fuzzy system using the DAMADICS model," in *International Conference on Applied Automation and Industrial Diagnostics* (U. of Djelfa, ed.), (Algeria), p. 0185, March 2015.

[10] S. Yin, S. X. Ding, A. Haghani, H. Hao, and P. Zhang, "A comparison study of basic data-driven fault diagnosis and process monitoring methods on the benchmark Tennessee Eastman process," *Journal of Process Control*, vol. 22, pp. 1567–1581, 2012. https://doi.org/10.1016/j.jprocont.2012.06.009

[11] A. Kowsalya and B. Kannapiran, "Principal component analysis based approach for fault diagnosis in pneumatic valve using DAMADICS benchmark simulator," *International Journal of Research in Engineering and Technology*, vol. 3(7), pp. 702–707, 2014. https://doi.org/10.15623/IJRET.2014.0319125

[12] F. J. Uppal, R. J. Pattona, and M. Witczak, "A neuro-fuzzy multiple-model observer approach to robust fault diagnosis based on the DAMADICS benchmark problem," *Control Engineering Practice*, vol. 14, 2006. https://doi.org/10.1016/j.conengprac.2005.04.015

[13] J. Ding, R. Alroobaea, A. M. Baqasah, A. Althobaiti, R. Miglani, H. S. Gill, "Big bata intelligent collection and network failure analysis based on artificial intelligence," *Informatica*, vol. 46, pp. 383-392, 2022. https://doi.org/10.31449/inf.v46i3.3866

[14] S. Xiong, L. Zhou, Y. Dai, and X. Ji, "Attention-based long short-term memory fully convolutional network for chemical process fault diagnosis," *Chinese Journal of Chemical Engineering*, vol. 56, pp. 1-14, 2022.https://doi.org/10.1016/j.cjche.2022.06.029

[15] R. Qin and J. Zhao, "Adaptive multiscale convolutional neural network model for chemical process fault diagnosis," *Chinese Journal of Chemical Engineering*, vol. 50, pp. 398–411, 2022. https://doi.org/10.1016/j.cjche.2022.10.001

[16] G. C. Silva, E. E. O. Carvalho, and W. M. Caminhas, "An artificial immune systems approach to case-based reasoning applied to fault detection and diagnosis," *Expert Systems with Applications*, vol. 140, p. 112906, 2020. https://doi.org/10.1016/j.eswa.2019.112906

[17] Z. Xie, J. Chen, Y. Feng, and S. He, "Semi-supervised multi-scale attention-aware graph convolution network for intelligent fault diagnosis of machine under extremely-limited labeled samples," *Journal of Manufacturing Systems*, vol. 64, pp. 561–

577, 2022. https://doi.org/10.1016/j.jmsy.2022.08.007

[18] G. Hong and D. Suh, "Mel spectrogram-based advanced deep temporal clustering model with unsupervised data for fault diagnosis," *Expert Systems With Applications*, vol. 217, p. 119551, 2023. https://doi.org/10.1016/j.eswa.2023.119551

[19] Y. Xu, X. Zeng, S. Bernard, and Z. He, "Data-driven prediction of neutralizer pH and valve position towards precise control of chemical dosage in a wastewater treatment plant," *Journal of Cleaner Production*, vol. 348, p. 131360, 2022. https://doi.org/10.1016/j.jclepro.2022.131360

[20] M. Bartyś, R. Patton, M. Syfert, S. de las Heras, and J. Quevedo, "Introduction to the DAMADICS actuator FDI benchmark study," *Control Engineering Practice*, vol. 14(6), no. 6, pp. 577–596, 2006. https://doi.org/10.1016/j.conengprac.2005.06.015

[21] P. Subbaraj and B. Kannapiran, "Fault detection and diagnosis of pneumatic valve using adaptive neuro-fuzzy inference system approach," *Applied Soft Computing*, vol. 19, pp. 362–371, 2014. https://doi.org/10.1016/j.asoc.2014.02.008

[22] D. Saravanakumar, B. Mohan, and T. Muthuramalingam, "A review on recent research trends in servo pneumatic positioning systems," *Precision Engineering*, vol. 49, pp. 481–492, 2017. https://doi.org/10.1016/j.precisioneng.2017.01.014

[23] S.-H. Wang, T.-W. Ni, and Z.-G. Yang, "Failure analysis on abnormal blockage of electro-hydraulic servo valve in digital electric hydraulic control system of 125 MW thermal power plant," *Engineering Failure Analysis*, vol. 123, p. 105294, 2021. https://doi.org/10.1016/j.engfailanal.2021.105294

[24] K. Zhang, J. Yao, and T. Jiang, "Degradation assessment and life prediction of electro-hydraulic servo valve under erosion wear," *Engineering Failure Analysis*, vol. 36, pp. 284–300, 2014. https://doi.org/10.1016/j.engfailanal.2013.10.017

[25] J. Shi, J. Yi, Y. Ren, Y. Li, Q. Zhong, H. Tang, and L. Chen, "Fault diagnosis in a hydraulic directional valve using a two-stage multi-sensor information fusion," *Measurement*, vol. 179, p. 109460, 2021. https://doi.org/10.1016/j.measurement.2021.109460

[26] F. Khan, M. T. Amin, V. Cozzani, and G. Reniers, *Methods in Chemical Process Safety*, ch. Domino effect: Its prediction and prevention - An overview, pp. 1–35. Elsevier, 2021. https://doi.org/10.1016/bs.mcps.2021.05.001

[27] U. Pal, G. Mukhopadhyay, and S. Bhattacharya, "Failure analysis of spring of hydraulic operated valve," *Engineering Failure Analysis*, vol. 95, pp. 191–198, 2019. https://doi.org/10.1016/j.engfailanal.2018.09.013

[28] G. M. de Almeida and S. W. Park, "Fault detection and diagnosis in the DAMADICS benchmark actuator system - a hidden Markov model approach," *IFAC Proceedings Volumes*, vol. 41(2), no. 2, pp. 12419–12424, 2008. 17th IFAC World Congress. https://doi.org/10.3182/20080706-5-KR-1001.02102

[29] R. B. di Capaci and C. Scali, "Review and comparison of techniques of analysis of valve stiction: From modeling to smart diagnosis," *Chemical Engineering Research and Design*, vol. 130, pp. 230–265, 2018. https://doi.org/10.1016/j.cherd.2017.12.038

[30] V. Puig, A. Stancu, and J. Quevedo, "Robust fault isolation using non-linear interval observers: The DAMADICS benchmark case study," in *16th Triennial World Congress* (Elsevier, ed.), (Prague, Czech Republic), pp. 293–298, 2005. https://doi.org/10.3182/20050703-6-CZ-1902.01851

[31] R. Babuška, *Fuzzy Modeling for Control*. Aachen, Germany: International Series in Intelligent Technologies, 1998. https://doi.org/10.1007/978-94-011-4868-9

[32] A. Lemos, W. Caminhas, and F. Gomide, "Adaptive fault detection and diagnosis using an evolving fuzzy classifier," *Information Science*, vol. 220, pp. 64–85, 2013. https://doi.org/10.1016/j.ins.2011.08.030

[33] Y. Kourd, D. Lefebvre, and N. Guersi, "FDI with neural network models of faulty behaviours and fault probability evaluation: Application to DAMADICS," in *Supervision and Safety of Technical Processes* (I. F. of Automatic Control, ed.), (Mexico City, Mexico), pp. 744–749, August 2012. https://doi.org/10.3182/20120829-3-MX-2028.00106

[34] J. Sarkar, Z. H. Prottoy, M. T. Bari, and M. A. A. Faruque, "Comparison of ANFIS and ANN modeling for predicting the water absorption behavior of polyurethane treated polyester fabric," *Heliyon*, vol. 7(9), no. 9, p. e08000, 2021. https://doi.org/10.1016/j.heliyon.2021.e08000

[35] V. Gomathi, V. Elakkiya, R. Valarmathi, and K. Ramkumar, "Actuator fault detection using adaptive neuro fuzzy approach for DAMADICS benchmark," *Research Journal of Pharmaceutical, Biological and Chemical Sciences*, vol. 7(1), no. 1, pp. 628–635, 2016.

[36] A. Andrade, K. Lopes, B. Lima, and A. Maitelli, "Development of a methodology using artificial neural network in the detection and diagnosis of faults for pneumatic control valves," *Sensors*, vol. 21, p. 853, 2021. https://doi.org/10.3390/s21030853

[37] A. R. C. Oliveira and J. M. G. S. da Costa, "Hierarchic fault diagnosis by pattern - recognition approaches applied to DAMADICS benchmark," in *18th World Congress The International Federation of Automatic Control* (I. F. of Automatic Control, ed.), (Milano, Italy), pp. 7737–7742, August 2011. https://doi.org/10.3182/20110828-6-IT-1002.03638

[38] A. Katunin, M. Amarowicz, and P. Chrzanowski, "Faults diagnosis using self-organizing maps: A case study on the DAMADICS benchmark problem," in *Federated Conference on Computer Science and Information Systems*, pp. 1673–1681, 2015. https://doi.org/10.15439/2015F26

[39] T. Chopra and J. Vajpai, "Classification of faults in DAMADICS benchmark process control system using self organizing maps," *International Journal of Soft Computing and Engineering*, vol. 1(3), no. 3, pp. 85–90, 2011.

[40] V. Palade, C. D. Bocaniala, and L. Jain, *Computational Intelligence in Fault Diagnosis*. Advanced Information and Knowledge Processing, United States of America: Springer-Verlag London, 2006.

[41] C. D. Bocaniala and V. Palade, *Computational intelligence methodologies in fault diagnosis: Review and state of the art, Computational intelligence in fault diagnosis*, ch. Computational intelligence methodologies in fault diagnosis: Review and state of the art, pp. 1–36. United States of America: Springer-Verlag London, 2006. https://doi.org/10.1007/978-1-84628-631-5_1

[42] P. Supavatanakul, J. Lunze, V. Puig, and J. Quevedo, "Diagnosis of timed automata: Theory and application to the DAMADICS actuator benchmark problem," *Control Engineering Practice*, vol. 14, pp. 609–619, 2006. https://doi.org/10.1016/j.conengprac.2005.03.028

[43] C. Gomes-Bezerra, B. S. Jales-Costa, L. A. Guedes, and P. P. Angelov, "An evolving approach to unsupervised and real-time fault detection in industrial processes," *Expert Systems With Applications*, vol. 63, pp. 134–144, 2016. https://doi.org/10.1016/j.eswa.2016.06.035

[44] X. Li, X. Yang, Y. Yang, I. Bennett, and D. Mba, "A novel diagnostic and prognostic framework for incipient fault detection and remaining service life prediction with application to industrial rotating machines," *Applied Soft Computing*, vol. 82, p. 105564, 2019. https://doi.org/10.1016/j.asoc.2019.105564

[45] Y. Langeron, A. Grall, and A. Barros, "Actuator lifetime management in industrial automation," *IFAC Proceedings Volumes*, vol. 45(20), no. 20, pp. 642–647, 2012. https://doi.org/10.3182/20120829-3-MX-2028.00111

[46] R. Kosturkov, V. Nachev, and T. Titova, "Diagnosis of pneumatic systems on basis of time series and generalized feature for comparison with standards for normal working condition," *TEM Journal*, vol. 10(1), no. 1, pp. 183–191, 2021. https://api.semanticscholar.org/CorpusID:233904474

[47] J. Yang and C. Delpha, "An incipient fault diagnosis methodology using local Mahalanobis distance: Fault isolation and fault severity estimation," *Signal Processing*, vol. 200, p. 108657, 2022. https://doi.org/10.1016/j.sigpro.2022.108657

[48] M. A. Márquez-Vera, L. E. Ramos-Velasco, O. López-Ortega, N. S. Zúñiga-Peña, J. C. Ramos-Fernández, and R. M. Ortega-Mendoza, "Inverse fuzzy fault model for fault detection and isolation with least angle regression for variable selection," *Computers & Industrial Engineering*, vol. 159, p. 107499, 2021. https://doi.org/10.1016/j.cie.2021.107499

[49] J. Vosloo, K. R. Uren, G. van Schoor, L. Auret, and H. Marais, "Exergy-based fault detection on the Tennessee Eastman process," *IFAC-PapersOnLine*, vol. 53(2), no. 2, pp. 13713–13720, 2020. https://doi.org/10.1016/j.ifacol.2020.12.875

[50] L. Zhang and K. Li, "Forward and backward least angle regression for nonlinear system identification," *Automatica*, vol. 53, pp. 94–102, 2015. https://doi.org/10.1016/j.automatica.2014.12.010

[51] R. Fazai, M. Mansouri, K. Abodayeh, H. Nounou, and M. Nounou, "Online reduced kernel PLS combined with GLRT for fault detection in chemical systems," *Process Safety and Environmental Protection*, vol. 128, pp. 228–243, 2019. https://doi.org/10.1016/j.psep.2019.05.018

[52] F. Cannarile, M. Compare, P. Baraldi, G. Diodati, V. Quaranta, and E. Zio, "Elastic net multinomial logistic regression for fault diagnostics of on-board aeronautical systems," *Aerospace Science and Technology*, vol. 94, p. 105392, 2019. https://doi.org/10.1016/j.ast.2019.105392

[53] H. Lee, C. Kim, S. Lim, and J. M. Lee, "Data-driven fault diagnosis for chemical processes using transfer entropy and graphical LASSO," *Computers & Chemical Engineering*, vol. 142, p. 107064, 2020.

https://doi.org/10.1016/j.compchemeng.2020.107064

[54] T. Ross, *Fuzzy Logic with Engineering Applications*. West Sussex: John Wiley & Sons, Ltd., 2008.

[55] M. A. Márquez-Vera, J. C. Ramos-Fernández, L. F. Cerecero-Natale, F. Lafont, J.-F. Balmat, and J. I. Esparza-Villanueva, "Temperature control in a MISO greenhouse by inverting its fuzzy model," *Computers and Electronics in Agriculture*, vol. 124, pp. 168–174, 2016. https://doi.org/10.1016/j.compag.2016.04.005

[56] D. Faouzi, "Optimization, modeling and simulation of microclimate and energy management of the greenhouse by modeling the associated heating and cooling systems and implemented by a fuzzy logic controller using artificial intelligence," *Informatica*, vol. 41, pp. 317-331.

[57] M. Bartys and M. Syfert, *Using Damadics Actuator Benchmark Library*. Warsaw University if Technology, 00-661 Warsaw, Poland, 1.22 ed., April 2002. Simulink Library Help File.

[58] X. M. Zhang and Q. L. Han, "Output feedback stabilization of networked control systems with a logic zero-order-hold," *Information Sciences*, vol. 381, pp. 78–91, 2017. https://doi.org/10.1016/j.ins.2016.11.009

[59] H. Dimassi, "A novel fault reconstruction and estimation approach for a class of systems subject to actuator and sensor faults under relaxed assumptions," *ISA Transactions*, vol. 111, pp. 192–210, 2021. https://doi.org/10.1016/j.isatra.2020.10.063

[60] H. Kazemi and A. Yazdizadeh, "Fault reconstruction in a class of nonlinear systems using inversion-based filter," *Nonlinear Dynamics*, vol. 85, pp. 1805–1814, 2016. https://doi.org/10.1007/s11071-016-2796-z

[61] A. R. Várkonyi-Kóczy, A. Álmos, and T. Kovácsházy, "Genetic algorithms in fuzzy model inversion," in *International Fuzzy Systems Conference Proceedings* (IEEE, ed.), (Seul, Korea), pp. 1421–1426, August 1999. https://doi.org/10.1109/FUZZY.1999.790112

[62] M. Shakarami and K. Esfandiari, "Rapid fault reconstruction using a bank of sliding mode observers," *Journal of the Franklin Institute*, vol. 359(18), pp. 11229-11255, 2022. https://doi.org/10.1016/j.jfranklin.2022.09.012

[63] U. Libal and Z. Hasiewicz, "Wavelet based rule for fault detection," *IFAC PapersOnLine*, vol. 51(24), pp. 255–262, 2018. https://doi.org/10.1016/j.ifacol.2018.09.585

[64] M. Jalayer, C. Orsenigo, and C. Vercellis, "Fault detection and diagnosis for rotating machinery: A model based on convolutional LSTM, fast Fourier and continuous wavelet transforms," *Computers in Industry*, vol. 125, p. 103378, 2021. https://doi.org/10.1016/j.compind.2020.103378

[65] Z. Feng and X. Chen, "Adaptive iterative generalized demodulation for nonstationary complex signal analysis: Principle and application in rotating machinery fault diagnosis," *Mechanical Systems and Signal Processing*, vol. 110, pp. 1–27, 2018. https://doi.org/10.1016/j.ymssp.2018.03.004

[66] V. M. Pukhova, T. V. Kustov, and G. Ferrini, "Time-frequency analysis of non-stationary signals," in *Conference of Russian Young Researchers in Electrical and Electronic Engineering* (IEEE, ed.), (Moscow and St. Petersburg, Russia), pp. 1141–1145, January 2018. 10.1109/IVForum.2017.8246088

[67] C. Li, Y. Huang, and L. Zhu, "Color texture image retrieval based on Gaussian copula models of Gabor wavelets," *Pattern Recognition*, vol. 64, pp. 118–129, 2017. https://doi.org/10.1016/j.patcog.2016.10.030

[68] K. Vernekar, H. Kumar, and K. V. Gangadharan, "Gear fault detection using vibration analysis and continuous wavelet transform," *Procedia Materials Science*, vol. 5, pp. 1846–1852, 2014. https://doi.org/10.1016/j.mspro.2014.07.492

[69] K. Yan and X. Zhou, "Chiller faults detection and diagnosis with sensor network and adaptive 1D CNN," *Digital Communications and Networks*, vol. 8, pp. 531–539, 2022. https://doi.org/10.1016/j.dcan.2022.03.023

[70] W. M. Salilew, Z. A. A. Karim, and T. A. Lemma, "Investigation of fault detection and isolation accuracy of different machine learning techniques with different data processing methods for gas turbine," *Alexandria Engineering Journal*, vol. 61(12), no. 12, pp. 12635–12651, 2022. https://doi.org/10.1016/j.aej.2022.06.026